PCCP

Accepted Manuscript

This is an *Accepted Manuscript*, which has been through the Royal Society of Chemistry peer review process and has been accepted for publication.

Accepted Manuscripts are published online shortly after acceptance, before technical editing, formatting and proof reading. Using this free service, authors can make their results available to the community, in citable form, before we publish the edited article. We will replace this *Accepted Manuscript* with the edited and formatted *Advance Article* as soon as it is available.

You can find more information about *Accepted Manuscripts* in the Information for Authors.

Please note that technical editing may introduce minor changes to the text and/or graphics, which may alter content. The journal's standard Terms & Conditions and the Ethical guidelines still apply. In no event shall the Royal Society of Chemistry be held responsible for any errors or omissions in this *Accepted Manuscript* or any consequences arising from the use of any information it contains.

ROYAL SOCIETY OF CHEMISTRY

www.rsc.org/pccp

Journal Name

RSCPublishing

ARTICLE

Geometry Controls the Stability of $FeSi_{14}$

Cite this: DOI: 10.1039/xoxxoooooox

Vikas Chauhan, Marissa Baddick Abreu, Arthur C. Reber, and Shiv N. Khanna [a]

Received ooth January 2012,
Accepted ooth January 2012

DOI: 10.1039/xoxxoooooox

www.rsc.org/

First-principles theoretical studies have been carried out to investigate the stability of Si_n cages impregnated with a Fe atom. It is shown that $FeSi_9$, $FeSi_{11}$, and $FeSi_{14}$ clusters exhibit enhanced local stability as seen through an increase in Si binding energy, Fe embedding energy, the gap between the Highest Occupied Molecular Orbital (HOMO) and the Lowest Unoccupied Molecular Orbital (LUMO), and the Ionization Potential (IP). The conventional picture for the stability of such species combines an assumption of electron precise bonding with the 18-electron rule; however, we find this to be inadequate to explain the enhanced stability in $FeSi_{11}$ and $FeSi_{14}$ because the d-band is filled for all $FeSi_n$ clusters for $n \geq 9$. $FeSi_{14}$ is shown to be the most stable due to a compact and highly symmetric Si_{14} cage with octahedral symmetry that allows better mixing between Fe 3d- and Si 3p- electronic states.

Introduction

Silicon and carbon belong to the same periodic group, but, while both atoms have four valence electrons, they exhibit different bonding patterns. Diamond is an insulator while Si is a semiconductor. On the nanoscale, C forms stable graphene sheets and cages. Silicon, however, prefers sp^3 bonding, favors tetrahedral coordination, and does not form graphitic sheets or fullerene cages. The structure of silicon clusters has been the subject of intense research over the past 25 years and it is now known that in contrast to bulk Si, small clusters often have complex structures with Si sites of varying coordination.[1–4] In particular, it was suggested that silicon cages with low coordinated Si sites could be stabilized by introducing metal atoms.[5–7] These clusters could be assembled into materials with tunable properties[8,9] and could result in magnetic silicon when brought together which could be highly valuable to the electronics industry.[10,11] This generated considerable interest in studies of silicon cages with endohedral metal atoms and theoretical studies reported such cages to be quite stable.[12,13] The clusters' stability was experimentally confirmed by Hiura, Kanayama, and co-workers, who generated a series of hydrogenated silicon clusters by reacting silane with several 5d transition metal atoms.[14] Through an examination of the relative intensities of MSi_n^+, $MSi_nH_2^+$, and $MSi_nH_4^+$ clusters in the reacted beam, these authors proceeded to identify the unusually stable (magic) species. In particular, for the WSi_n clusters, the non-reactivity with silane and the preponderance of WSi_{12} prompted Hiura et al. to argue that WSi_{12} is a highly stable magic species. Hiura et al. also proposed that the stability of WSi_{12} could be rationalized within the 18-electron rule, assuming that each Si atom contributes one electron to the valence of W, which already has six electrons.

The suggestion of the 18-electron rule as a guiding principle for WSi_{12} prompted a flurry of theoretical activity, much of it focused on its isoelectronic congener $CrSi_{12}$.[15–30] The application of the 18-electron rule is based on the electron precise bonding between Si and the transition metal where each Si contributes one electron to the valence pool. Other models based on a confined nearly free electron gas have also been proposed.[24–34]

In a recent paper, we revisited the applicability of the 18-electron rule to $CrSi_n$ clusters and, in particular, the reported stability of $CrSi_{12}$.[35] Our investigations, based on first-principles density functional calculations, showed that the ground state structure of $CrSi_{12}$ is an oblate hexagonal prism with a Cr site occupying an interior location, in agreement with numerous previous studies.[14,15,20,24,32,36–39] More importantly, a critical examination of the bonding showed that the electronic structure of $CrSi_{12}$ does not conform to the 18-electron rule. An analysis of the electronic states with appreciable Cr character revealed that $CrSi_{12}$ has only 16 effective valence electrons assigned to the Cr atom and an unoccupied $3d_z^2$ orbital. The oblate D_{6h} structure leads to a large crystal field-like splitting of the 3d-orbitals, which results in an appreciable HOMO-LUMO gap, enabling the cluster to exhibit some of the attributes of stable clusters. The addition of two Si atoms to form $CrSi_{14}$ leads to the filling of the 3d-states in accordance with the 18-electron rule, and $CrSi_{14}$ exhibits all conventional markers of a magic cluster. The geometric structure of $CrSi_{14}$ has a Cr site surrounded by a compact (C_{2v}) Si_{14} cage that leads to a close grouping of the Cr 3d-states and suppresses the crystal field

Physical Chemistry Chemical Physics Accepted Manuscript

splitting seen in $CrSi_{12}$. The cluster has a larger number of Si-Si bonds and favors better mixing between Cr 3d- and Si 3p-states. While these studies provided some support for the 18-electron rule, the compact $CrSi_{14}$ cage structure raises the question as to whether the geometry plays an important role in the stability. Recent work by Goicoechea and McGrady also suggests that the geometry of the Si cage and the bonding between silicon atoms is just as important to consider as the filling of the d-states on the metal atom.[40] One way to explore this is to examine MSi_n clusters with a metal M that has a different number of valence electrons.

The purpose of the present paper is to carry out first-principles studies on $FeSi_n$ clusters containing up to 16 Si atoms. Fe has two more valence electrons than Cr and one would expect a filled $3d_z^2$ orbital in $FeSi_{12}$; however, if the structure is driven by stabilizing the Fe core, the cluster would likely find a more compact Si cage encapsulating the atom, while if cage bonding plays a dominant role, then the same structure will be found. Furthermore, if the electronic effects are dominant, $FeSi_{12}$ should be highly stable. On the other hand, if the geometric effects are dominant, one would expect $FeSi_{14}$ with a symmetrical cage to be more stable, assuming that the cluster has the same structure as $CrSi_{14}$. To critically assess the role of geometric factors on stability, we analyzed the connectivity of the Si_n cage (number of Si-Si bonds) as a function of size. We find that the 18-electron rule does not explain the stability of the $FeSi_n$ clusters identified in this work, because all of the clusters $n \geq 9$ have fully occupied 3d-shells, yet large variations in stability are found. Thus, the stability of these larger $FeSi_n$ clusters cannot be reconciled within the 18-electron rule. In particular, we show that the bonding is not electron precise and that the geometry of the cage plays an important role by controlling the mixing between the transition metal and silicon electronic states.

Method

Density functional theory studies were carried out on $FeSi_n$ (n = 6-16) using the generalized gradient approximation (GGA) for exchange and correlation as proposed by Perdew, Burke, and Ernzerhof (PBE).[41,42] We previously showed this to be an accurate functional for the $CrSi_n$ clusters by comparison of simulated and experimental photoelectron spectra.[35] Actual calculations were completed using the Amsterdam Density Functional (ADF) set of codes,[43,44] in which the atomic wave functions are expressed in terms of Slater-type orbitals (STO) located at the atomic sites. The cluster wave functions are constructed from a linear combination of these atomic orbitals. A TZ2P basis set and a small frozen electron core [$1s^2$ $2s^2$ $2p^6$] was used for both Si and Fe atoms.[45] Scalar relativistic effects were incorporated using the Zero-Order Regular Approximation[46–48] to allow for comparison with larger transition metal atoms. Numerous initial geometries were tried in order to cover the potential energy surface. The calculations covered the neutral as well as anionic and cationic species, and several possible spin multiplicities were considered for all clusters.

Result and discussion

Fig. 1 shows the ground state geometries, including spin multiplicities, of neutral $FeSi_n$ (n=6-16) clusters, with the higher energy isomers given in Fig. S1(a-f). These structures are similar to the ones obtained in previous theoretical studies.[18,20,24,28,32,38,49]

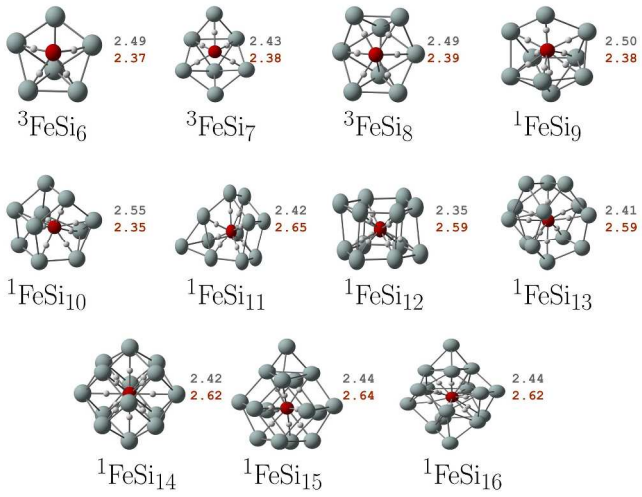

Fig. 1 Ground State structures of neutral $FeSi_n$ (n = 6-16) clusters. Si and Fe atoms are shown in gray and dark red, respectively. Superscripts indicate the multiplicities (M=2S+1) of the clusters. The average bond lengths are shown for Si-Si in gray and Fe-Si in red. Bond critical points are also shown by white dummy atoms.

The ground states of $FeSi_6$, $FeSi_7$, and $FeSi_8$ are spin triplet and the Fe sites carry spin magnetic moments, an indication that the d-states are not filled. From $FeSi_9$ onwards the ground states are all spin singlet as the Fe spin moment is quenched. For $FeSi_{10}$, a spin triplet state is marginally more stable than the ground state by 0.007 eV, as shown in Fig. S1(c), but here we have chosen to focus on the singlet configuration as it relates to larger species. For smaller sizes, the Fe site is exposed to the outside, but as the size increases, Fe occupies an interior site that is completely surrounded by Si atoms. Complete encapsulation occurs at $FeSi_{10}$. The geometry of $FeSi_{12}$ is similar to the oblate D_{6h} cage found for $CrSi_{12}$, but is slightly distorted. $FeSi_{14}$ is found to have a structure even more symmetric than $CrSi_{14}$, with the most stable structure being a rhombic dodecahedron with O_h symmetry that is 0.43 eV more stable than the C_{2v} structure of $CrSi_{14}$. $FeSi_{14}$ is also the largest cluster in which every Si atom is bound to the encapsulated Fe atom. Fig. 1 also shows average Si-Si and Fe-Si bond lengths, and we find that the average Fe-Si bond length increases with size.

In order to uncover clusters with enhanced stability, we calculated several energetic properties, including: the energy gain, ΔSi, as a Si atom is added to the preceding size; the embedding energy, ΔFe, representing the gain in energy as a Fe atom is added to a Si_n cluster; the HOMO-LUMO gap; the

Physical Chemistry Chemical Physics Accepted Manuscript

This journal is © The Royal Society of Chemistry 2012

vertical and adiabatic detachment energies (VDE and ADE), the energy differences between the anionic ground state and a neutral cluster in the geometry of the anion and in its ground state geometry, respectively; and the vertical and adiabatic ionization potentials (VIP and AIP), the energy differences between the neutral ground state and cationic cluster in the geometry of the neutral and in its ground state geometry, respectively. Some of these energies are defined by

$$\Delta Si = (E(FeSi_{n-1}) + E(Si)) - E(FeSi_n) \quad (1)$$
$$\Delta Fe = (E(Si_n) + E(Fe)) - E(FeSi_n) \quad (2)$$
$$ADE = E(FeSi_n^-) - E(FeSi_n) \quad (3)$$
$$AIP = E(FeSi_n^+) - E(FeSi_n) \quad (4)$$

Here $E(FeSi_n)$, $E(FeSi_n^+)$, and $E(FeSi_n^-)$ are the total energies of the ground state neutral, cationic, and anionic $FeSi_n$ cluster, respectively, while E(Si) and E(Fe) are the total energies of the Si and Fe atoms, respectively. $E(Si_n)$ is the total energy of the ground state of the pure Si_n (n = 6-16) clusters previously reported,[35] which agree with other theoretical studies.[1–4] The ground states of the anions and cations used for the calculation of ADE/VDE and AIP/VIP are shown in Figs. S2 and S3 of the Supplemental Information.

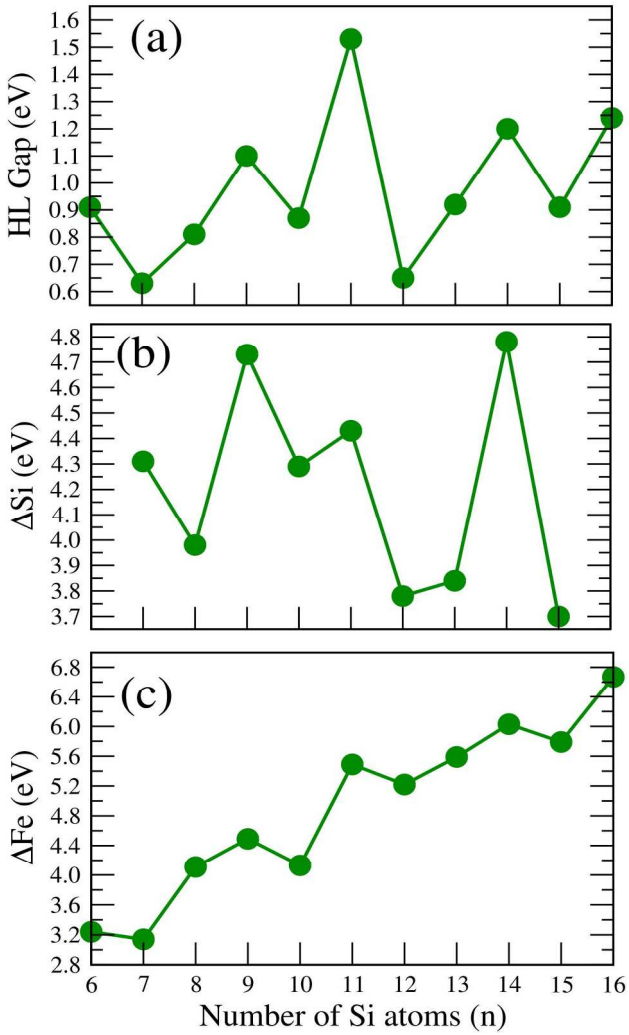

Fig. 2 (a) HOMO-LUMO gap (b) Silicon binding energy, ΔSi, for n=7-16, and (c) Iron embedding energy, ΔFe. All the values are given in eV.

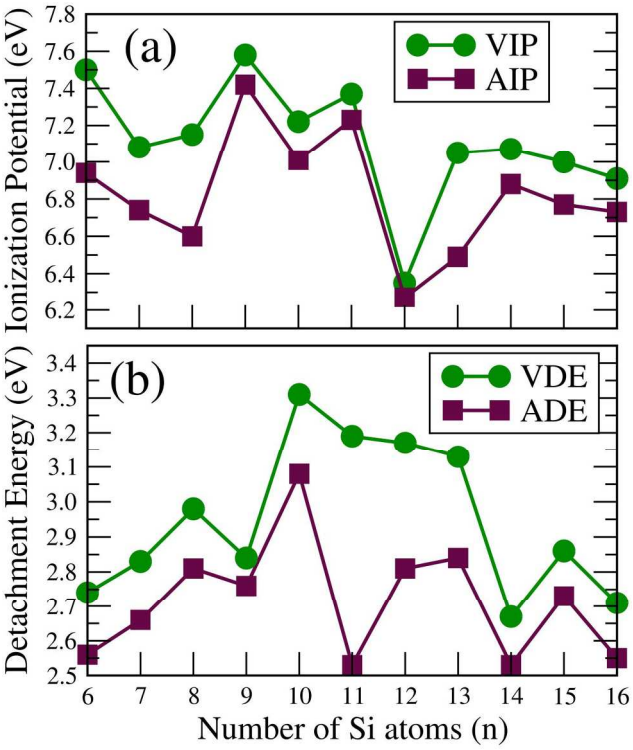

Fig. 3 (a) Vertical and adiabatic ionization potential (b) Vertical and adiabatic detachment energy for n=6-16. All the values are given in eV.

In Fig. 2, we present the HOMO-LUMO gaps, ΔSi, and ΔFe. Table S1 in the Supplemental Information provides the numerical values for all energetic properties. From Fig. 2(a), it is clear that $FeSi_9$, $FeSi_{11}$, and $FeSi_{14}$ all show local maxima for the HOMO-LUMO gap. For each of these clusters, the gap is higher than 1.1 eV. Our previous studies have shown that clusters with a gap higher than 1.1 eV are generally resilient to reacting with etchants like oxygen and hence can be regarded as chemically stable.[50] The clusters are also energetically stable as indicated by variations in ΔSi and ΔFe. For ΔSi, $FeSi_9$, $FeSi_{11}$, and $FeSi_{14}$ are marked by a gain in energy of 4.4 eV - 4.8 eV in growing the clusters from previous size. These clusters also show a drop in binding in growing to the next size. The variations in ΔFe are less obvious. On average, ΔFe increases with size as the Fe site bonds to a growing number of Si atoms; however, there are local jumps at $FeSi_9$, $FeSi_{11}$, and $FeSi_{14}$, indicating their enhanced stability.

To further determine if the special stability at $FeSi_9$, $FeSi_{11}$, and $FeSi_{14}$ depends on electronic features, we present the VIP, AIP, VDE, and ADE in the Fig. 3. While the AIPs show local maxima at $FeSi_9$, $FeSi_{11}$, and $FeSi_{14}$, local maxima are found only at $FeSi_9$ and $FeSi_{11}$ for VIP. Note that similar local maxima are seen at magic sizes for metal clusters and are usually a signature of shell closings. The other signature of shell closure is the minima in binding of an electron when added to such clusters. Indeed, the ADE shows local minima at these sizes. The trends in the VDE are less noticeable since it is primarily determined by the ground state of the anionic species.

Physical Chemistry Chemical Physics Accepted Manuscript

As previously discussed, application of the 18-electron rule coupled with the assumption of electron precise bonding wherein each Si contributes an electron to the valence of Fe would suggest a maximum stability at $FeSi_{10}$ since Fe has 8 valence electrons. However, $FeSi_{10}$ and $FeSi_{12}$ do not show any signs of enhanced stability. In comparing the geometry of $FeSi_{12}$ to that of $CrSi_{12}$, the hexagonal prism formed by the two faces is distorted in $FeSi_{12}$, which suggests that the filling of $3d_z^2$ orbital in the Fe core results in a symmetry breaking and lower symmetry structure than the D_{6h} of $CrSi_{12}$. To further determine if the filling of the metal d-shell through bonding with Si atoms is associated with the observed stability at $FeSi_9$, $FeSi_{11}$, and $FeSi_{14}$, we analyzed the electronic states in the $FeSi_n$ clusters. To get a quantitative picture, we calculated the percentage of d_z^2, d_{xy}, d_{yz}, d_{xz}, and $d_{x^2-y^2}$ in all the occupied orbitals for sizes ranging from $FeSi_8$ to $FeSi_{15}$ using a Mulliken population analysis. Numerical values of d-state contributions are given in the Table S2. Fig. 4 shows these percentages from $FeSi_8$ through $FeSi_{15}$. Since the Fe 3d-states bond with Si 3s- and 3p-states, we regarded those states that have more than 50% population as effectively filled states (if the bonding states are occupied, we would expect around 50% population). Note that d_Z^2 and d_{yz} in the minority spin states of $FeSi_8$ have less than 50% occupation and so could be regarded as unfilled. From $FeSi_9$ on, all of the clusters may be considered to have filled 3d orbitals, and there is no apparent difference in the 3d occupation of the magic sizes and the non-magic sizes. $FeSi_9$ has the second largest ΔSi energy, a relatively large HOMO-LUMO gap, and a local maximum in the ΔFe energy, consistent with being the smallest cluster to which the 18-electron rule applies. However, when analyzing the stability of all clusters larger than n=9, the role of the 18-electron rule is not clear as it applies to all of these clusters. This reveals that bonding with Si fills the 3d-shell of Fe more easily than the electron precise model prediction that previous studies have suggested. Thus, some other factor must be driving the magic stability of $FeSi_{14}$. In an attempt to see if the additional stability was associated with the pure Si_n cages, we calculated ΔSi for pure Si_n clusters. Enhanced values for ΔSi are observed at n = 10, 12, and 14. While the magic sizes at 9 and 11 do not correspond to any of these numbers, the stability of $FeSi_{14}$ might have common origin.

From a fundamental point of view, these clusters are composed of Si-Si and Fe-Si interactions, and so we surveyed trends in these interactions with increasing cluster size. We first investigated the number of Si atoms that are actually bonded to Fe through an examination of bond critical points (BCPs). A point (r_c) in the 3-dimensional electron density (ρ) distribution where the gradient of ρ vanishes is known as a critical point (CP). Particularly, the behaviour of ρ near r_c is characterized by the rank R and signature of S of the CP. These two indices (R, S) are obtained by diagonalizing the Hessian matrix of ρ. The rank R is the number of non-zero eigenvalues and S is the algebraic sum of the signs of the eigenvalues indicating the topological feature (i.e. maxima, minima or saddle) of the CP. The (3, -1) CP indicates a saddle point in electron density

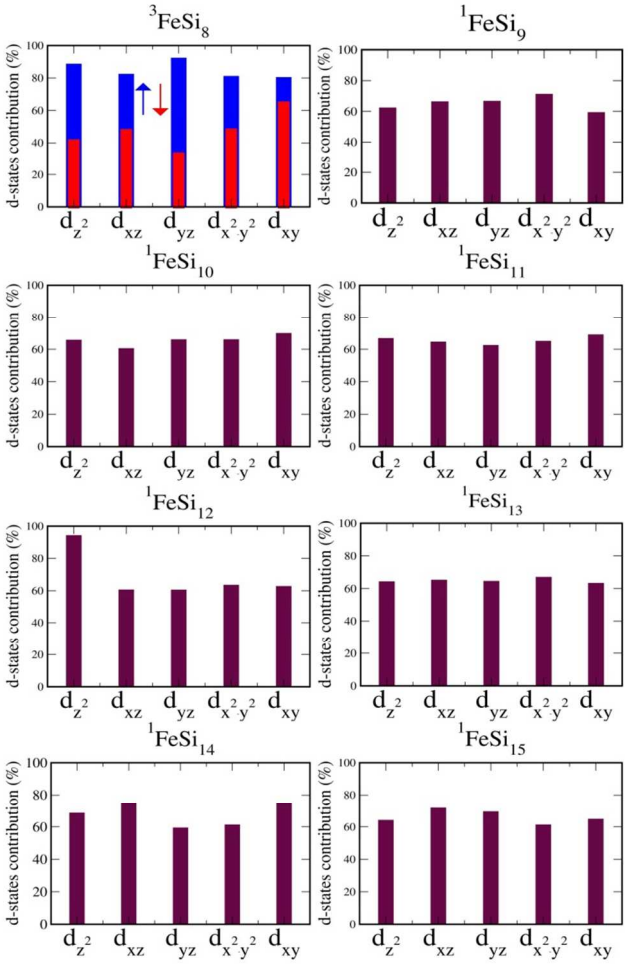

Fig. 4 The Fe d-states contributions (%) in the $FeSi_n$ (n=8-15) clusters. The blue and red bars show the contributions in majority and minority spin states, respectively, for $FeSi_8$. The purple bars indicate the contributions in both spin states for n=9-15.

distribution and is observed when a pair of atoms are bonded in a given cluster or molecule. Therefore, it is named the bond critical point.[51,52] Fig. 5(a) shows the number of BCPs between Fe and Si atoms as a function of size. It is interesting that the trend in the number of Fe-Si BCPs has jumps at 9, 11, and 14, indicating that the metal becomes bonded to more Si atoms at these sizes. We also note that there is a local maximum in the number of BCPs at 12, which is due to the cluster's highly symmetric nearly D_{6h} atomic structure. To further characterize the bonding, we inspected the connectivity of the Si_n cage by calculating the number of Si-Si bonds (NSS). Fig. 5(b) shows the variation of the NSS with size. Note that there is an increase in NSS at 9, 11, and 14, indicating that the connectivity of the cage does increase at stable sizes. While the variations in BCPs and NSS provide some guidance to the observed magic sizes, a more physical picture into how these changes affect the stability is needed. Recently, it has been suggested that aromaticity plays a role in stabilizing cage and encapsulating cage clusters.[53] NICS is the most common measure of aromaticity.[54] Since $FeSi_{14}$ is found to be a highly symmetric, we have evaluated the NICS values at various positions as

Physical Chemistry Chemical Physics Accepted Manuscript

This journal is © The Royal Society of Chemistry 2012

shown in Fig. S8. All the NICS values (Table S2) are found to be negative; however, the presence of charge density also causes a negative NICS value making it difficult to determine if this is due to ring currents or simple bonding. Generally, NICS is an indicator of stability at the center of the cage, and we do find that the Si_{14} cage has a NICS value of -41.9 ppm, consistent with a stable cage structure.[55]

To develop a more conceptual basis, we further investigated the bonding between Fe and Si sites by examining the variations in the overlap partial density of states (OPDOS), which can provide information about the nature of the bonding

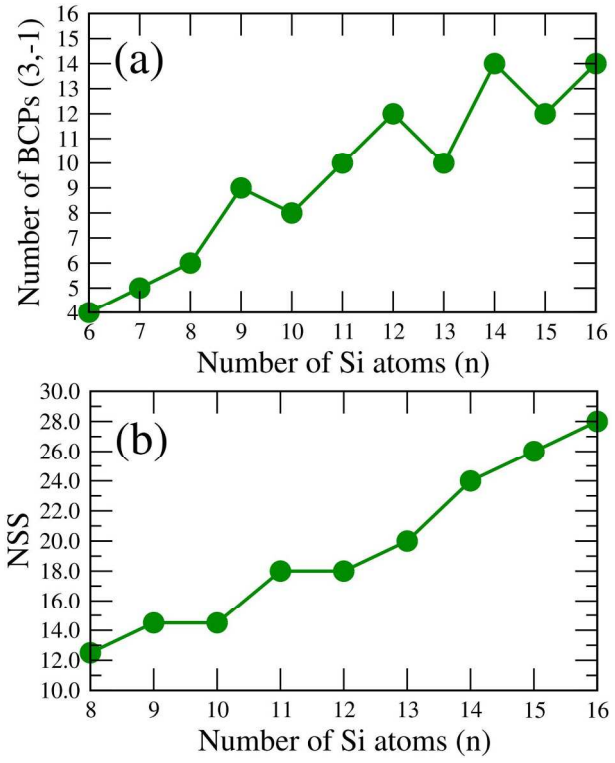

Fig. 5 (a) Bond critical points (BCPs) and (b) number of Si-Si bonds (NSS) in $FeSi_n$ (n=8-16) clusters.

(a positive OPDOS corresponds to bonding interaction and a negative OPDOS corresponds to anti-bonding), the strength of mixing, and the location of bonding and anti-bonding states in energy. Figs. S4 through S6 in the Supplemental Information show the OPDOS for $FeSi_8$ through $FeSi_{16}$ clusters. Since $FeSi_8$ has a triplet ground state, the figure shows the OPDOS for both the spins. Starting with $FeSi_8$ and $FeSi_9$, the filled states are bonding states. $FeSi_{10}$ has an anti-bonding state near HOMO that is unfilled. At $FeSi_{11}$, the anti-bonding states begin to be occupied and the number of anti-bonding states increases with size. For $FeSi_{14}$, the bonding states are grouped closely due to the cluster's high symmetry. The anti-bonding state is located at the HOMO and so does not adversely affect the stability.

As the OPDOS includes all the states, we identified the states with significant hybridization between the Fe d-states and the Si sp-states. In Fig. 6 we present (1) the location of the LUMO, (2) the location of the HOMO, and (3) the width of the d-band through energy spread of the states with appreciable contribution from Fe 3d-orbitals. One notices that there is significant variation in the width of the d-band. A smaller width of the d-band results from a more spherical distribution of Si atoms around the Fe core, assuming that the d-band is fully occupied. Thus, the width of the d-band can provide information abound the local geometry of Si surrounding Fe. For most sizes, the states are fairly spread out. However, for $FeSi_9$, $FeSi_{11}$, and $FeSi_{14}$, the d-band narrows to 0.53, 0.88, and 0.05 eV, respectively. This effect is most pronounced for $FeSi_{14}$ due to its highly symmetric octahedral structure with a nearly spherical distribution of Si atoms around the Fe core. At these sizes, the variation in the energy of the HOMO also shows a local minimum. For $FeSi_{14}$, which has the largest ΔSi, a high HOMO-LUMO gap and embedding energy, and low ADE and VDE, we additionally find large connectivity as seen through NSS, a high number of BCPs between Fe and Si atoms, the narrowest d-band, strong hybridization between the Fe d-states and Si sp-states, and anti-bonding character that is pushed to the HOMO. All of these factors lead to a highly stable species.

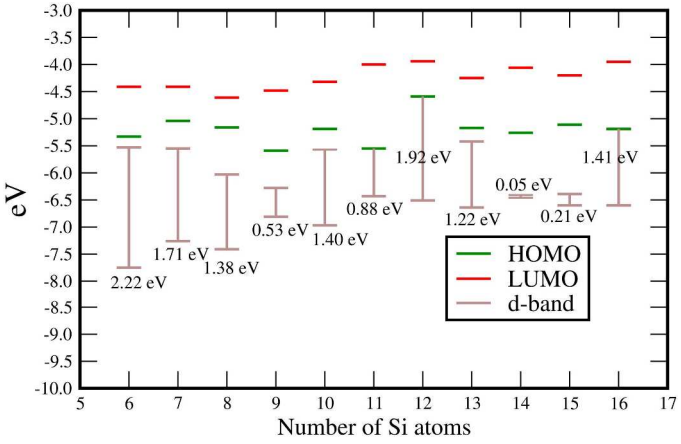

Fig. 6 The variation in d-band width and position of the HOMO and LUMO in $FeSi_n$ (n=6-16) clusters. The d-band width is given in eV.

Conclusion

The above results point to a more unified picture for the stability of $FeSi_n$ clusters. The stability has contributions from the Si-Si bonds in that the magic sizes have marked increases in connectivity and hence the number of such bonds. This is reasonable as Si-Si bonds contribute to the increase in energy. An associated effect is the increase in metal-Si bonds. The analysis of the bond critical points indicates that the more stable species have a higher number of BCPs, which leads to an increase in silicon binding energy. The other significant effect, however, is the mixing between the Fe 3d- and Si p-states. The cages that are more spherical allow for an effective mixing between the states and lead to narrower bands of bonding states, which results in an increase in bonding and the emergence of special magic sizes. Our studies find that the stability enhancement brought on by the filling of the transition

Physical Chemistry Chemical Physics Accepted Manuscript

metal d-bands occurs at $FeSi_9$, which has fewer silicon atoms than that predicted by previous electron precise counting rules. Rather, the stability of $FeSi_{14}$ is caused by the cluster's octahedral cage structure, which maximizes bonding between the Fe atom and the Si cage. We hope that the present findings would encourage experimental investigations of the spectroscopy and other properties for transition metal doped silicon clusters.

Acknowledgement

We gratefully acknowledge funding support from the Department of Energy under Award Number DE-SC0006420.

Notes and references

[a]Department of Physics, Virginia Commonwealth University, 701 West Grace Street, Richmond, Virginia 23284-2000, United States Fax:804-828-7073; Tel:804-828-1820; E-mail: snkhanna@vcu.edu

Electronic Supplementary Information (ESI) available: Higher energy isomers of neutral $FeSi_n$ clusters, geometries of anions and cations, OPDOS, table of energetic property values, XYZ coordinates for neutral clusters. See DOI: 10.1039/b000000x/

1 M. Iwamatsu, *J. Chem. Phys.*, 2000, **112**, 10976.
2 K.-M. Ho, A. A. Shvartsburg, B. Pan, Z.-Y. Lu, C.-Z. Wang, J. G. Wacker, J. L. Fye and M. F. Jarrold, *Nature*, 1998, **392**, 582–585.
3 C. M. Rohlfing and K. Raghavachari, *Chem. Phys. Lett.*, 1990, **167**, 559–565.
4 M. A. Belkhir, S. Mahtout, I. Belabbas and M. Samah, *Phys. E Low-Dimens. Syst. Nanostructures*, 2006, **31**, 86–92.
5 S. M. Beck, *J. Chem. Phys.*, 1987, **87**, 4233–4234.
6 S. M. Beck, *J. Chem. Phys.*, 1989, **90**, 6306–6312.
7 K. Jackson and B. Nellermoe, *Chem. Phys. Lett.*, 1996, **254**, 249–256.
8 S. A. Claridge, A. W. Castleman, S. N. Khanna, C. B. Murray, A. Sen and P. S. Weiss, *ACS Nano*, 2009, **3**, 244–255.
9 S. Mandal, A. C. Reber, M. Qian, P. S. Weiss, S. N. Khanna and A. Sen, *Acc. Chem. Res.*, 2013.
10 R. Robles and S. N. Khanna, *J. Chem. Phys.*, 2009, **130**, 164313.
11 R. Robles and S. N. Khanna, *Phys. Rev. B*, 2009, **80**, 115414.
12 V. Kumar and Y. Kawazoe, *Phys. Rev. Lett.*, 2001, **87**.
13 V. Kumar and Y. Kawazoe, *Phys. Rev. B*, 2002, **65**.
14 H. Hiura, T. Miyazaki and T. Kanayama, *Phys. Rev. Lett.*, 2001, **86**, 1733–1736.
15 S. Khanna, B. Rao and P. Jena, *Phys. Rev. Lett.*, 2002, **89**.
16 A. N. Andriotis, G. Mpourmpakis, G. E. Froudakis and M. Menon, *New J. Phys.*, 2002, **4**, 78.
17 G. Mpourmpakis, G. E. Froudakis, A. N. Andriotis and M. Menon, *Phys. Rev. B*, 2003, **68**, 125407.
18 P. Sen and L. Mitas, *Phys. Rev. B*, 2003, **68**, 155404.
19 C. Sporea and F. Rabilloud, *J. Chem. Phys.*, 2007, **127**, 164306.
20 J. Lu and S. Nagase, *Phys. Rev. Lett.*, 2003, **90**.
21 F. Hagelberg, C. Xiao and W. Lester, *Phys. Rev. B*, 2003, **67**, 035426.
22 H. Kawamura, V. Kumar and Y. Kawazoe, *Phys. Rev. B*, 2004, **70**, 245433.
23 A. Negishi, N. Kariya, K. Sugawara, I. Arai, H. Hiura and T. Kanayama, *Chem. Phys. Lett.*, 2004, **388**, 463–467.
24 J. Ulises Reveles and S. Khanna, *Phys. Rev. B*, 2005, **72**.
25 K. Koyasu, J. Atobe, M. Akutsu, M. Mitsui and A. Nakajima, *J. Phys. Chem. A*, 2007, **111**, 42–49.
26 P. Gruene, A. Fielicke, G. Meijer, E. Janssens, V. T. Ngan, M. T. Nguyen and P. Lievens, *ChemPhysChem*, 2008, **9**, 703–706.
27 J. Li, G. Wang, C. Yao, Y. Mu, J. Wan and M. Han, *J. Chem. Phys.*, 2009, **130**, 164514–164514–9.
28 J. He, K. Wu, C. Liu and R. Sa, *Chem. Phys. Lett.*, 2009, **483**, 30–34.
29 P. Claes, E. Janssens, V. T. Ngan, P. Gruene, J. T. Lyon, D. J. Harding, A. Fielicke, M. T. Nguyen and P. Lievens, *Phys. Rev. Lett.*, 2011, **107**, 173401.
30 K. Koyasu, M. Akutsu, M. Mitsui and A. Nakajima, *J. Am. Chem. Soc.*, 2005, **127**, 4998–4999.
31 N. Uchida, T. Miyazaki and T. Kanayama, *Phys. Rev. B*, 2006, **74**, 205427.
32 J. Ulises Reveles and S. N. Khanna, *Phys. Rev. B*, 2006, **74**, 035435.
33 W. D. Knight, K. Clemenger, W. A. de Heer, W. A. Saunders, M. Y. Chou and M. L. Cohen, *Phys. Rev. Lett.*, 1984, **52**, 2141–2143.
34 W. Ekardt, *Phys. Rev. B*, 1984, **29**, 1558–1564.
35 M. B. Abreu, A. C. Reber and S. N. Khanna, *J. Phys. Chem. Lett.*, 2014, **5**, 3492–3496.
36 T. Miyazaki, H. Hiura and T. Kanayama, *Phys. Rev. B*, 2002, **66**, 121403.
37 H. Kawamura, V. Kumar and Y. Kawazoe, *Phys. Rev. B*, 2004, **70**.
38 L. Guo, G. Zhao, Y. Gu, X. Liu and Z. Zeng, *Phys. Rev. B*, 2008, **77**.
39 X. Kong, H.-G. Xu and W. Zheng, *J. Chem. Phys.*, 2012, **137**, 064307.
40 J. E. McGrady and J. M. Goicoechea, *Dalton Trans.*, 2015.
41 J. P. Perdew, K. Burke and M. Ernzerhof, *Phys. Rev. Lett.*, 1996, **77**, 3865.
42 J. P. Perdew, K. Burke and M. Ernzerhof, *Phys. Rev. Lett.*, 1997, **78**, 1396–1396.
43 C. F. Guerra, J. G. Snijders, G. Te Velde and E. J. Baerends, *Theor. Chem. Acc.*, 1998, **99**, 391–403.
44 G. te Velde, F. M. Bickelhaupt, E. J. Baerends, C. Fonseca Guerra, S. J. A. van Gisbergen, J. G. Snijders and T. Ziegler, *J. Comput. Chem.*, 2001, **22**, 931–967.
45 E. Van Lenthe and E. J. Baerends, *J. Comput. Chem.*, 2003, **24**, 1142–1156.
46 E. van Lenthe, E. J. Baerends and J. G. Snijders, *J. Chem. Phys.*, 1993, **99**, 4597–4610.
47 E. van Lenthe, E. J. Baerends and J. G. Snijders, *J. Chem. Phys.*, 1994, **101**, 9783–9792.
48 E. van Lenthe, A. Ehlers and E.-J. Baerends, *J. Chem. Phys.*, 1999, **110**, 8943–8953.
49 S. N. Khanna, B. K. Rao, P. Jena and S. K. Nayak, *Chem. Phys. Lett.*, 2003, **373**, 433–438.
50 A. C. Reber, S. N. Khanna, P. J. Roach, W. H. Woodward and A. W. Castleman, *J Am Chem Soc*, 2007, **129**, 16098–16101.
51 R. F. W. Bader, *Atoms in Molecules - A Quantum Theory*, Oxford University Press, New York, 1990.

Physical Chemistry Chemical Physics Accepted Manuscript

 This journal is © The Royal Society of Chemistry 2012

52 D. Bandyopadhyay, P. Kaur and P. Sen, *J. Phys. Chem. A*, 2010, **114**, 12986–12991.
53 R. Trivedi, K. Dhaka and D. Bandyopadhyay, *RSC Adv*, 2014, **4**, 64825–64834.
54 P. von R. Schleyer, C. Maerker, A. Dransfeld, H. Jiao and N. J. R. van E. Hommes, *J. Am. Chem. Soc.*, 1996, **118**, 6317–6318.
55 P. A. Clayborne, U. Gupta, A. C. Reber, J. J. Melko, S. N. Khanna and A. W. Castleman, *J. Chem. Phys.*, 2010, **133**, 134302.

Physical Chemistry Chemical Physics Accepted Manuscript